Received: 18 December 2019 | Revised: 22 February 2020 | Accepted: 23 February 2020

DOI: 10.1002/aoc.5657

Applied Organometallic Chemistry WILEY

FULL PAPER

CeO_2/CuO@N-GQDs@NH_2 nanocomposite as a high-performance catalyst for the synthesis of benzo[g] chromenes

Javad Safaei-Ghomi | **Fatemeh-Sadat Bateni** | **Pouria Babaei**

Department of Organic Chemistry, Faculty of Chemistry, University of Kashan, Kashan, 51167, I. R, Iran

Correspondence
Javad Safaei-Ghomi, Department of Organic Chemistry, Faculty of Chemistry, University of Kashan, Kashan, 51167, I. R. Iran.
Email: safaei@kashanu.ac.ir

A three-component reaction of aromatic aldehydes, malononitrile or ethyl cyanoacetate and 2-hydroxy-1,4-naphthaquinone has been achieved in the presence of an amino-functionalized CeO_2/CuO@ nitrogen graphene quantum dot nanocomposite as a highly effective heterogeneous catalyst to produce benzo[g]chromenes. The catalyst has been characterized by X-ray diffraction, scanning electron microscopy, transmission electron microscopy, Fourier transform infrared, energy-dispersive X-ray spectroscopy, thermogravimetric analysis, X-ray photoelectron spectroscopy, Brunauer-Emmett-Teller (BET) and vibrating sample magnetometry. This new catalyst has been demonstrated to be highly effective in the preparation of benzo[g]chromenes.

KEYWORDS

chromenes, graphene quantum dots, nanocatalyst, nanocomposite

1 | INTRODUCTION

Chromenes have biological properties including anticancer,[1] antimicrobial,[2] antivirus,[3] anti-inflammatory[4] and antidiabetes,[5] and are used in the treatment of Alzheimer's disease.[6] Some other examples of chromenes are prominent drug molecules such as vitamin E, acronycine, uvafzlelin and cromakalim, which have high bioavailability, slow onset and prolonged effect.[7] Chromenes are regarded as notable targets of organic synthesis. Therefore, searching for efficient methods for the preparation of chromenes is an attractive challenge. A number of methods have been developed for the preparation of chromenes using diverse catalysts containing lipase,[8] *p*-TSA,[9] Et_3N,[10] Zn[L-proline]$_2$,[11] $[Et_3NH][HSO_4]$,[12] DBU,[13] Cu $(OTf)_2$,[14] TEBA (triethylbenzylammonium chloride)[15] and [bmim]OH.[16] Metal oxides are a broad class of materials that have been researched extensively owing to their unique attributes and potential applications in various fields.[17, 18] Graphene quantum dots (GQDs) have received much attention owing to their significant features regarding biological,[19] biomedical,[20] drug delivery,[21] photocatalyst,[22] surfactant,[23] bioelectronic,[24] electrocatalytic,[25] Li-ion battery,[26] solar cell,[27] photoluminescence[28,29] and bioimaging properties,[30] and catalytic activity.[31] Potential applications of *N*-GQDs have been reviewed on the basis of theoretical and experimental studies.[32–35] Herein, we report on the use of a CeO_2/CuO@N-GQDs@NH_2 nanocomposite as a new and efficient catalyst for the preparation of benzo[g]chromenes through a three-component reaction of aromatic aldehydes, malononitrile or ethyl cyanoacetate and 2-hydroxy-1,4-naphthaquinone (Scheme 1).

2 | EXPERIMENTAL SECTION

2.1 | Preparation of CeO_2/CuO nanoparticles

Ce $(SO_4)_2{\cdot}4H_2O$ and $CuCl_2{\cdot}2H_2O$ with 1:1 molar ratio were dissolved in deionized water. Afterwards, the

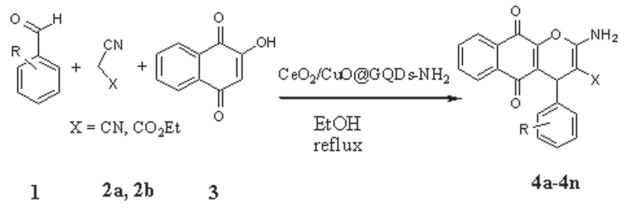

SCHEME 1 Synthesis of benzo[g]chromenes using CeO_2/CuO@N-GQDs@NH_2 nanocomposite

appropriate amount of aqueous sodium hydroxide solution (0.70 M) was added to the solution until the pH value reached 10. Then, the transparent solution was placed in an autoclave at 120°C for 6 h. The obtained precipitate was washed twice with methanol and dried at 60°C for 5 h. Finally, the product was calcined at 500°C for 2 h.

2.2 | Preparation of CeO_2/CuO@N-GQDs nanocomposite

A 1 g aliquot of citric acid was dissolved into 20 ml deionized water, and stirred to form a clear solution. After that, 0.3 ml ethylenediamine was added to the above solution and mixed to obtain a clear solution. Then, 0.1 g CeO_2/CuO nanoparticles were added to mixture. The mixture was stirred at room temperature for 5 min. Then the solution was transferred into a 50 ml Teflon-lined stainless autoclave. The sealed autoclave was heated to 180°C for 9 h in an electric oven. Finally, as-prepared nanostructured CeO_2/CuO@N-GQDs were obtained, washed several times with deionized water and ethanol, and then dried in an oven until a constant weight was achieved.

2.3 | Preparation of CeO_2/CuO@N-GQDs@NH_2 nanocomposite

A 1 g aliquot of CeO_2/CuO@N-GQDs nanocomposite was added to a solution of 3-aminopropyltriethoxysilane (2 mmol, 0.44 g) in dry toluene (20 ml) and refluxed for 24 h under N_2 atmosphere. After the reaction had finished, the aminated CeO_2/CuO@N-GQDs were separated using a centrifuge, washed with double-distilled water and anhydrous ethanol, and dried at 80°C for 8 h to give the surface-bound amino group CeO_2/CuO@N-GQDs@NH_2.

2.4 | General procedure for the preparation of benzo[g]chromenes

A mixture of aldehyde (1 mmol), malononitrile (1 mmol), ethyl cyanoacetate (1 mmol), 2-hydroxy-1,-4-naphthaquinone (1 mmol) and 6 mg CeO_2/CuO@N-GQDs@NH_2 nanocomposite was stirred in 5 ml ethanol under reflux conditions. The reaction was monitored by TLC. After completion of the reaction, hot ethyl acetate was added. The catalyst was insoluble in ethyl acetate and it could therefore be recycled by simple filtration. Water was added, and the precipitate was collected by filtration and washed with water. The crude product was recrystallized or washed with ethanol to give the pure product. The structures of the products were confirmed using ^{1}H NMR and Fourier transform infrared (FT-IR) spectroscopy (see Supporting Information).

2.4.1 | *2-Amino-4-(4-chlorophenyl)-5,10-dihydro-5,10-dioxo-4H-benzo[g]chromene-3-carbonitrile* (4a)

Orange powder; m.p. 249–252°C. IR (KBr) (ν_{max}/cm^{-1}): 3406, 3419, 3336, 2199, 1666, 1529, 1355. ^{1}H NMR (400 MHz, DMSO-d_6): δ (ppm), 4.63 (1H, s, CH), 7.34–8.03 (10H, m, Ar and NH_2). ^{13}C NMR (100 MHz, DMSO-d_6): δ (ppm), 36.3, 57.6, 119.8, 121.7, 126.2, 126.4, 128.9, 130.2, 131.3, 131.5, 132.2, 134.6, 134.8, 143.1, 149.6, 158.8, 177.3, 182.6. Anal. calcd for $C_{20}H_{11}ClN_2O_3$: C, 66.22; H, 3.06; N, 7.72. Found: C, 66.12; H, 3.11; N, 7.79.

2.4.2 | *2-amino-4-(4-bromophenyl)-5,10-dihydro-5,10-dioxo-4H–benzo[g]chromene-3-carbonitrile* (4b)

Orange powder; m.p. 253–255°C. IR (KBr) (ν_{max}/cm^{-1}): 3410, 3195, 2200, 1664, 1596, 1347. ^{1}H NMR (400 MHz, DMSO-d_6): δ (ppm), 4.62 (1H, s, CH), 7.28–8.04 (10H, m, Ar and NH_2). ^{13}C NMR (100 MHz, DMSO-d_6): δ (ppm), 36.6, 57.5, 119.7, 120.6, 121.7, 126.3, 126.4, 130.2, 131.4, 131.6, 131.8, 134.5, 134.9, 143.5, 149.4, 158.6, 177.3, 183.1. Anal. calcd for $C_{20}H_{11}BrN_2O_3$: C, 58.99; H, 2.72; N, 6.88. Found: C, 58.92; H, 2.78; N, 6.78.

2.4.3 | *2-amino-4-(4-nitrophenyl)-5,10 -dihydro-5,10–dioxo-4H-benzo[g]chromene-3-carbonitrile* (4c)

Orange powder; m.p. 240–242°C. IR (KBr) (ν_{max}/cm^{-1}): 3418, 3332, 2199, 1666, 1595, 1529. ^{1}H NMR (400 MHz, DMSO-d_6): δ (ppm), 4.75 (1H, s, CH), 7.45–8.15 (10H, m, Ar and NH_2). ^{13}C NMR (100 MHz, DMSO-d_6): δ (ppm), 36.5, 56.9, 119.4, 121.2, 124.3, 126.3, 126.6, 129.7, 131.3, 131.5, 134.8, 135.2, 147.3, 149.8, 151.8, 158.7, 177.2, 182.7. Anal. calcd for $C_{20}H_{11}N_3O_5$: C, 64.35; H, 2.97; N, 11.26. Found: C, 64.25; H, 2.92; N, 11.20.

2.4.4 | *2-amino-5,10-dihydro-5,10-dioxo-4-phenyl-4H–benzo[g]chromene-3-carbonitrile* (4d)

Orange powder; m.p. 261–262°C. IR (KBr) (ν_{max}/cm^{-1}): 3457, 3392, 2213, 1662, 1592, 1406. ^{1}H NMR (400 MHz, DMSO-d_6): δ (ppm), 4.61 (1H, s, CH), 7.29–7.84 (11H, m, Ar and NH_2). ^{13}C NMR (100 MHz, DMSO- d_6): δ (ppm), 36.8, 57.6, 119.8, 122.5, 126.2, 126.5, 127.5, 128.3, 129.2, 131.1, 131.5, 134.7, 134.9, 144.0, 149.3, 158.7, 177.2, 183.3. Anal. calcd for $C_{20}H_{12}N_2O_3$: C, 73.16; H, 3.68; N, 8.53. Found: C, 73.09; H, 3.61; N, 8.59.

2.4.5 | *2-amino-4-(2-chlorophenyl)-5,10-dihydro-5,10-dioxo-4H-benzo[g]chromene-3-carbonitrile* (4e)

Orange powder, m.p. 237–239°C. IR (KBr) (ν_{max}/cm^{-1}): 3428, 2216, 1643, 1595. ^{1}H NMR (400 MHz, DMSO-d_6): δ (ppm), 4.81 (1H, s, CH), 7.23–8.06 (10H, m, Ar and NH_2). ^{13}C NMR (100 MHz, DMSO-d_6): δ (ppm), 33.8, 56.5, 119.3, 121.7, 126.3, 126.6, 128.4, 129.0, 129.7, 130.8, 131.1, 131.2, 132.6, 134.5, 135.5, 141.3, 149.7, 158.9, 177.4, 182.7. Anal. calcd for $C_{20}H_{11}ClN_2O_3$: C, 66.22; H, 3.06; N, 7.22. Found: C, 66.21; H, 3.02; N, 7.28.

2.4.6 | *Ethyl 2-amino-4-(4-nitrophenyl)-5, 10-dioxo-5, 10-dihydro-4H-benzo [g] chromene-3-carboxylate* (4f)

Orange solid; m.p.197–199°C. IR (KBr) cm^{-1}: 3408.14, 1681.02. ^{1}H NMR (400 MHz, $CDCl_3$): δ (ppm), 1.22 (t, 3H, J = 8.0 Hz), 4.08 (q, 2H, J = 8.0 Hz), 5.12 (s, 1H), 6.52 (s, 2H, NH_2), 7.53 (d, J = 7.2 Hz, 2H), 7.73–7.85 (d, J = 7.2 Hz, 2H), 8.14 (d, J = 8.0 Hz, 2H), 8.33 (d, J = 8.0 Hz, 2H). ^{13}C NMR (100 MHz,$CDCl_3$): δ (ppm), 14.4, 37.3, 61.9, 75.3, 120.8, 123.4, 126.3, 126.6, 130.5, 131.7, 135.9, 144.3, 150.8, 160.2, 162.3, 167.4, 178.5, 183.2. Anal. calcd for $C_{22}H_{16}N_2O_7$: C, 62.86; H, 3.84; N, 6.66. Found: C, 62.97; H, 3.94; N, 6.55%.

2.4.7 | *Ethyl2-amino-4-(3-nitrophenyl)-5,10-dioxo-5,10-dihydro-4H-benzo[g]chromene-3-carboxylate* (4g)

Orange solid; m.p. 198–200°C. IR (KBr) cm^{-1}: 3432.80, 1681.72. ^{1}H NMR (400 MHz,$CDCl_3$): δ (ppm), 1.27 (t, 3H, J = 8.0 Hz), 4.15 (q, 2H, J = 8.0 Hz), 5.11 (s, 1H), 6.63 (s, 2H, NH_2), 7.48 (m, 1H), 7.76 (m, 3H), 8.03 (m, 2H), 8.14 (m, 1H), 8.29 (s, 1H). ^{13}C NMR (100 MHz,$CDCl_3$): δ (ppm), 14.3, 36.7, 61.8, 75.4, 120.7, 120.8, 121.3, 121.7, 126.4, 130.3, 131.4, 134.6, 135.1, 145.8, 147.4, 160.7, 162.9, 167.4, 178.1, 183.2. Anal. calcd for $C_{22}H_{16}N_2O_7$: C, 62.86; H, 3.84; N, 6.66. Found: C, 62.95; H, 3.93; N, 6.52%.

2.4.8 | *Ethyl 2-amino- 4-(2-chlorophenyl)-5,10-dihydro-5,10-dioxo-4H-benzo [g] chromene-3-carboxylate* (4h)

Orange solid; m.p. 208–210°C. IR (KBr) cm^{-1}: 3432, 1681. ^{1}H NMR (400 MHz, DMSO- d_6): δ (ppm), 1.12 (t, 3H, J = 7.6 Hz), 3.92 (q, 2H, J = 7.6 Hz), 5.34 (s, 1H), 7.10 (s, 2H, NH_2), 7.14 (m, 1H),7.23 (m, 1H), 7.80–7.88 (m, 5H), 8.02 (m, 1H). ^{13}C NMR (100 MHz, DMSO-d_6): δ (ppm), 14.7, 32.2, 61.6, 75.3, 120.6, 126.3, 126.7, 126.7, 127.8, 128.4, 130.4, 131.5, 131.8, 135.3, 143.1, 160.4, 162.7, 167.4, 178.9, 183.8. Anal. calcd for $C_{22}H_{16}ClNO_5$: C, 64.48; H, 3.94; N, 3.42. Found: C, 64.46; H, 4.05; N, 3.54%.

2.4.9 | *Ethyl2-amino-4-(4-bromophenyl)-5,10-dioxo-5,10-dihydro-4H-benzo[g]chromene-3-carboxylate* (4i)

Orange solid; m.p. 190–192°C. IR (KBr) cm^{-1}: 3425.10, 1681.16. ^{1}H NMR (400 MHz, $CDCl_3$): δ (ppm), 1.22 (t, 3H, J = 7.6 Hz), 4.15 (q, 2H, J = 7.6 Hz), 5.12 (s,1H), 6.64 (s, 2H, NH_2), 7.24 (d, J = 7.6 Hz, 2H), 7.38 (d, J = 7.4 Hz, 2H), 7.72 (d, J = 8.2 Hz, 2H), 8.02 (d, J = 8.2 Hz, 1H), 8.15 (d, J = 7.4 Hz, 1H). ^{13}C NMR (100 MHz, $CDCl_3$): δ (ppm), 14.4, 37.8, 61.3, 75.7, 120.8, 120.8, 126.3, 130.5, 131.4, 131.7,131.8, 135.7, 143.4, 160.5, 162.4, 167.6, 178.5, 183.7. Anal. calcd for $C_{22}H_{16}BrNO_5$: C, 58.17; H, 3.55; N, 3.08. Found: C, 58.23; H, 3.60; N, 3.18%.

2.4.10 | *Ethyl 2-amino-4-(4-chlorophenyl)-5,10-dihydro-5,10-dioxo-4H-benzo[g]chromene-3-carboxylate* (4j)

Orange solid; m.p. 198–200°C. IR (KBr) cm^{-1}: 3461.46, 1681.56. ^{1}H NMR (400 MHz, $CDCl_3$): δ (ppm), 1.32 (t, 3H, J = 7.6 Hz), 4.22 (q, 2H, J = 7.6 Hz), 5.12 (s, 1H), 6.48 (s, 2H, NH_2), 7.20 (d, J = 7 Hz, 2H), 7.26 (d, J = 7 Hz, 3H), 7.65 (d, J = 8 Hz, 2H), 8.10–8.14 (d, J = 8 Hz, 1 H). ^{13}C NMR (100 MHz, $CDCl_3$): δ (ppm), 14.5, 37.4, 61.0, 75.9, 125.2, 126.2, 128.9, 130.7, 130.9, 131.5, 131.8, 135.4, 142.1, 160.1, 162.2, 167.3, 178.5, 183.9. Anal. calcd for $C_{22}H_{16}ClNO_5$: C, 64.48; H, 3.94; N, 3.42. Found: C, 64.40; H, 4.06; N, 3.58%.

2.4.11 | *Ethyl2-amino-4-(4-methoxyphenyl)-5,10-dioxo-5,10-dihydro-4H-benzo[g]chromene-3-carboxylate* (4k)

Orange solid; m.p. 223–225°C. IR (KBr) cm^{-1}: 3423.89, 1683.93. ^1H NMR (400 MHz,$CDCl_3$): δ (ppm), 1.25 (t, 3H, $J = 7.2$ Hz), 3.73 (s, 3H), 4.04 (q, 2H, $J = 7.2$ Hz), 5.26 (s, 1H), 6.34 (s, 2H, NH_2), 6.82 (d, $J = 8.2$ Hz, 1H), 6.92 (t, $J = 8.0$ Hz, 1H), 7.15 (t, 1H), 7.43 (d, $J = 7.2$ Hz, 1H),7.72 (m, 2H), 7.92 (m, 1H), 8.12 (m, 1H). ^{13}C NMR (100 MHz, $CDCl_3$): δ (ppm), 14.9, 31.4, 56.7, 61.4, 75.5, 112.8, 120.9, 121.7, 126.9, 127.1, 130.8, 131.6, 135.8, 158.5, 160.8, 162.7, 167.4, 178.5, 183.3. Anal. calcd for $C_{23}H_{19}NO_6$: C, 68.14; H, 4.72; N, 3.46. Found: C, 68.22; H, 4.74; N, 3.45%.

2.4.12 | *Ethyl 2-amino-4-(4-methylphenyl)-5,10-dihydro-5,10-dioxo-4H-benzo[g]chromene-3-carboxylate* (4l)

Yellow solid; m.p.212–214°C. IR (KBr) cm^{-1}: 3463.85, 1679.5. ^1H NMR (400 MHz, $CDCl_3$): δ (ppm), 1.25 (t, 3H, $J = 8.2$ Hz), 2.25 (s, 3H), 4.12 (q, 2H, $J = 8.2$ Hz), 5.16 (s, 1H), 6.43 (s, 2H, NH_2), 7.03 (d, $J = 7$ Hz, 2H), 7.23 (d, $J = 7$ Hz, 2H), 7.72 (d, $J = 8$ Hz, 2H), 8 (d, $J = 8$ Hz, 1H), 8.12 (d, J = 8 Hz, 1H). ^{13}C NMR (100 MHz,$CDCl_3$): δ (ppm), 14.9, 21.7, 37.2, 61.3, 75.8, 120.3, 126.4, 128.7,130.8, 131.5, 135.8, 135.8, 141.6, 160.5, 162.4, 167.8, 178.2, 183.7. Anal. calcd for $C_{23}H_{19}NO_5$: C, 70.94; H, 4.92, N; 3.60. Found: C, 70.90; H, 5.01; N, 3.68%.

2.4.13 | *2-amino-4-(furan-2-yl)-5,10-dihydro-5,10-dioxo-4H-benzo[g]chromene-3-carbonitrile* (4m)

Orange powder; m.p. 192–194°C. IR (KBr) (ν_{max}/cm^{-1}): 3409, 3425, 3334, 2198, 1660, 1525, 1354. ^1H NMR (400 MHz, DMSO-d_6): δ (ppm), 4.32 (1H, s, CH), 6.12–7.98 (9H, m, Ar and NH_2). ^{13}C NMR (100 MHz, DMSO-d_6): δ (ppm), 35.2, 57.4, 105.3, 111.4, 118.2, 126.3, 126.5, 130.6, 131.4, 132.2, 134.5, 134.8, 142.7, 149.2, 151.7, 158.2, 177.1, 181.5. Anal. calcd for $C_{18}H_{10}N_2O_4$: C, 67.92; H, 3.17; N, 8.80. Found: C, 67.82; H, 3.12; N, 8.72%.

2.4.14 | *2-amino-5,10-dihydro-5,10-dioxo-4-(thiophen-2-yl)-4H-benzo[g]chromene-3-carbonitrile* (4n)

Orange powder; m.p. 186–188°C. IR (KBr) (ν_{max}/cm^{-1}): 3402, 3421, 3332, 2195, 1667, 1528, 1359. ^1H NMR (400 MHz, DMSO-d_6): δ (ppm), 4.12 (1H, s, CH), 6.70–7.24 (9H, m, Ar and NH_2). ^{13}C NMR (100 MHz, DMSO-d_6): δ (ppm), 36.1, 57.2, 118.5, 122.8, 126.4, 126.6, 126.8, 127.9, 130.2, 131.4, 132.5, 134.1, 134.4, 142.5, 151.8, 158.3, 176.2, 182.1. Anal. calcd for $C_{18}H_{10}N_2O_3S$: C, 64.66; H, 3.01; N, 8.38. Found: C, 64.62; H, 3.08; N, 8.31%.

3 | RESULTS AND DISCUSSION

We prepared CeO_2/CuO nanoparticles by easy techniques. A hydrothermal way was used for the preparation of N-GQDs.[36] Amino-functionalized GQDs were prepared using 3-aminopropyltriethoxysilane. The X-ray diffraction (XRD) patterns of CeO_2/CuO and CeO_2/CuO@N-GQDs@NH_2 nanocomposite are shown in Figure 1. The XRD patterns confirm the presence of both CuO (JCPDS no. 89-2529) and CeO_2 (JCPDS no. 34-0394).

In order to investigate the morphology and particle size of nanocatalyst, scanning electron microscopy (SEM) images of CeO_2/CuO and CeO_2/CuO@N-GQDs@NH_2 nanocomposite are shown in Figure 2(a, b). Figure 2(c)

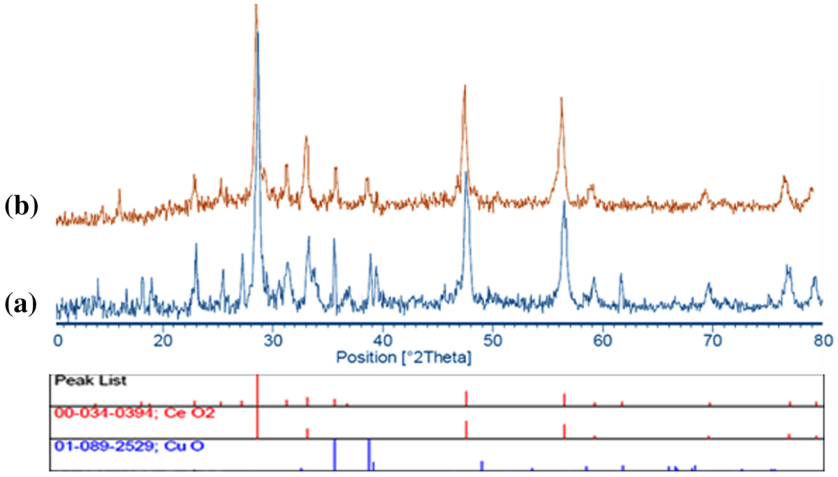

FIGURE 1 X-ray diffraction pattern of (a) CeO_2/CuO and (b) CeO_2/CuO@N-GQDs@NH_2

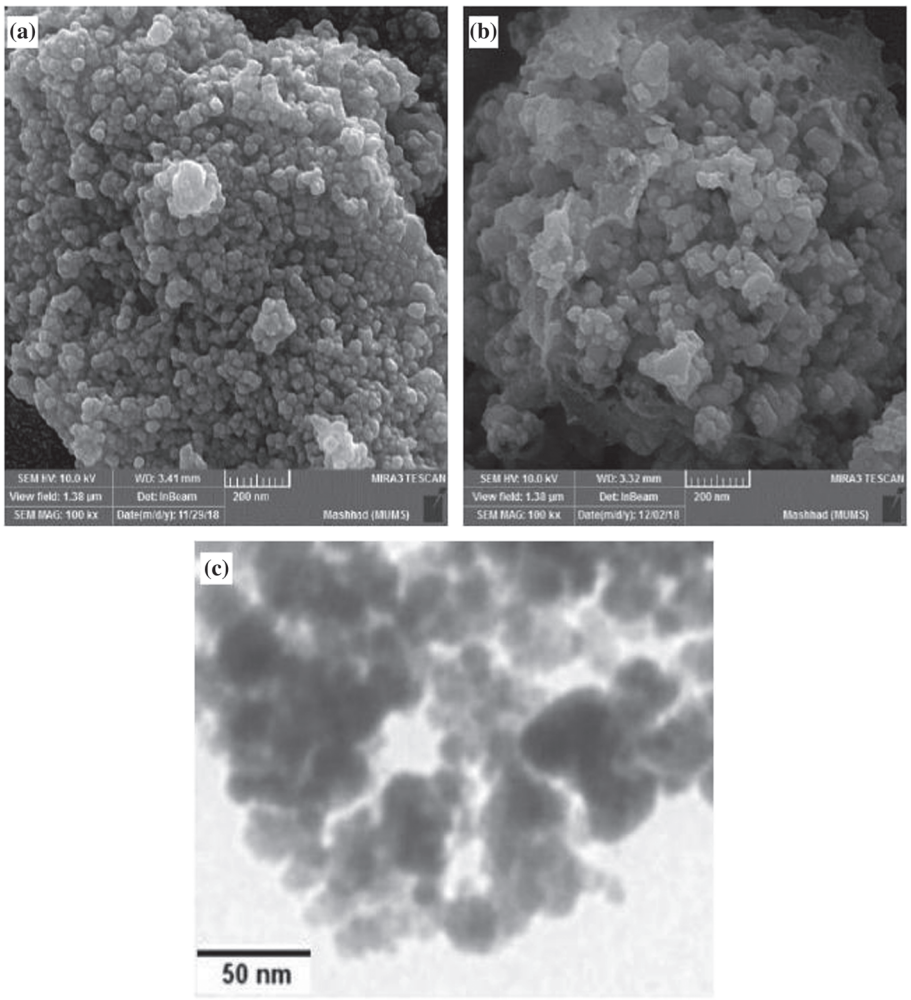

FIGURE 2 (a) Scanning electron microscopy (SEM) of CeO_2/CuO; (b) SEM of CeO_2/CuO@N-GQDs@NH_2; and (c) transmission electron microscopy of CeO_2/CuO@N-GQDs@NH_2

indicates the TEM (transmission electron microscope) image of nanocatalyst. The TEM and SEM images of the CeO_2/CuO@N-GQDs@NH_2 nanocomposite show the formation of uniform particles, and the energy-dispersive X-ray spectrum (EDS) confirms the presence of Ce, Cu, O, N and C species in the structure of the nanocomposite (Figure 3).

The magnetic properties of CeO_2/CuO, CeO_2/CuO@N-GQDs and CeO_2/CuO@N-GQDs@NH_2 nanocomposites were determined with the help of a

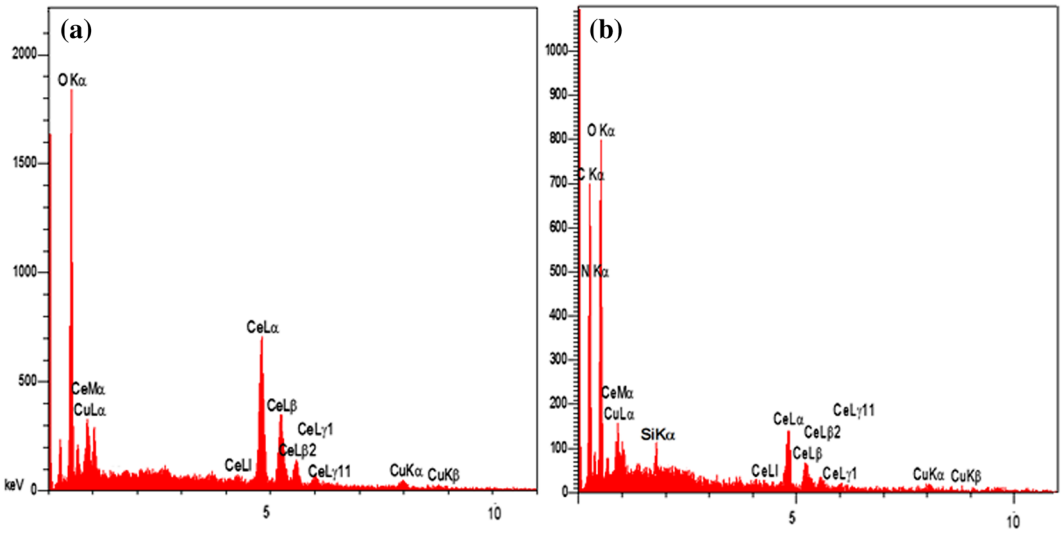

FIGURE 3 Energy-dispersive X-ray spectrum of (a) CeO_2/CuO and (b) CeO_2/CuO@-GQDs@NH_2

vibrating sample magnetometer (Figure 4). These results demonstrate that the magnetization property decreases with coating and functionalization.

The FT-IR spectra of CeO_2/CuO, CeO_2/CuO@N-GQDs and CeO_2/CuO@N-GQDs@NH_2 nanocomposites are shown in Figure 5. The absorption peak at 3300 cm^{-1} is related to the stretching vibrational absorptions of OH. The peaks at 509 and 663 cm^{-1} correspond to Cu–O and Ce–O respectively. The characteristic peaks at 3435 cm^{-1} (O-H stretching vibration), 1660 cm^{-1} (C=O stretching vibration) and 1101 cm^{-1} (C–O–C stretching vibration) appear in the spectrum shown in Figure 5b. The peak at approximately 1475–1580 cm^{-1} is attributed to C=C bonds. The peaks at 1560, 3438 and 3350 cm^{-1} are related to the bending and stretching vibrational absorptions of N–H (Figure 5c).

The BET specific surface areas of CeO_2/CuO and CeO_2/CuO@N-GQDs@NH_2 nanocomposites were measured using nitrogen gas adsorption–desorption isotherms (Figure 6). The results showed that the BET specific surface area of CeO_2/CuO improved from 1.72 to 9.82 m^2/g after modification with GQDs and 3-aminopropyltriethoxysilane; therefore, more active sites were introduced to the CeO_2/CuO@N-GQDs@NH_2 surface. The results for N_2 adsorption–desorption containing the BET surface area (S_{BET}) and the total pore volumes (V_{total}) of the CeO_2/CuO, CeO_2/CuO@N-GQDs and CeO_2/CuO@N-GQDs@NH_2 nanocomposites are summarized in Table 1.

Thermogravimetric analysis was used to examine the thermal stability of the CeO_2/CuO@N-GQDs@NH_2 nanocomposites (Figure 7). These nanoparticles show suitable thermal stability without a significant decrease in weight. The weight loss (2.14%) at temperatures below 200°C is due to the removal of physically adsorbed solvent and surface hydroxyl groups. The curve displays a weight loss of about 12.98% from 200 to 600°C, attributed to the oxidation and degradation of N-GQD and decomposition of the organic spacer grafting to the N-GQD surface.

X-ray photoelectron spectroscopy (XPS) analysis of CeO_2/CuO@N-GQDs@NH_2 nanocomposite is shown in

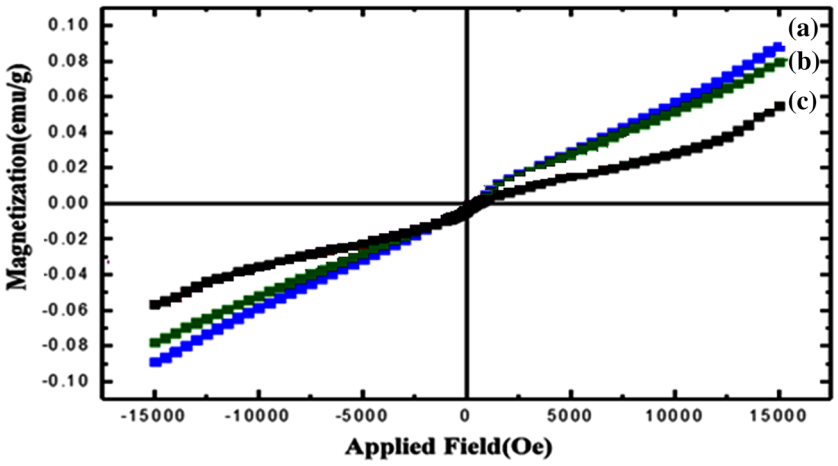

FIGURE 4 Vibrating sample magnetometer of (a) CeO_2/CuO, (b) CeO_2/CuO@GQDs and (c) CeO_2/CuO@GQDs@NH_2

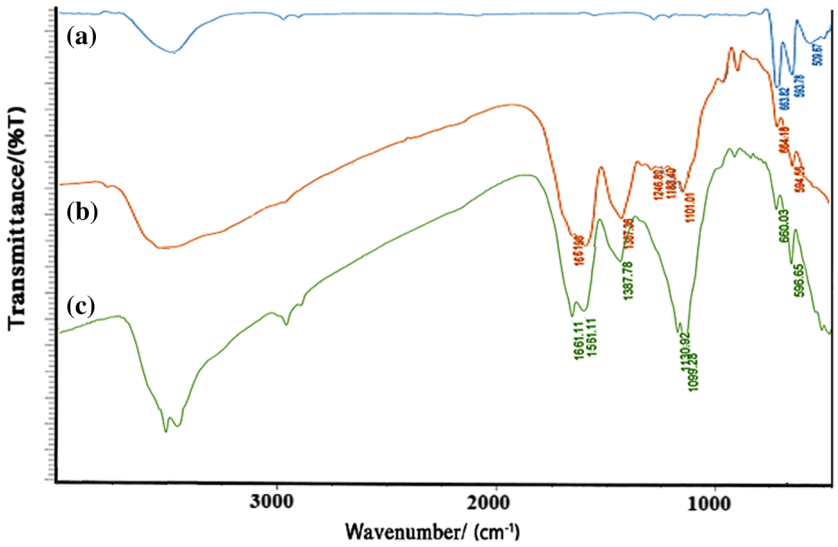

FIGURE 5 Fourier transform infrared spectrum of (a) CeO_2/CuO, (b) CeO_2/CuO@N-GQDs and (c) CeO_2/CuO@N-GQDs@NH_2

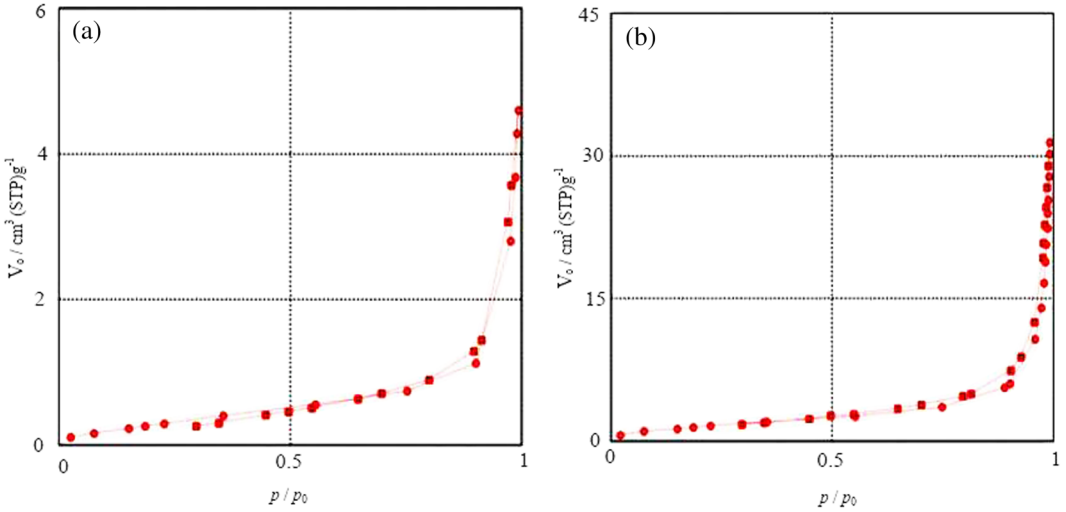

FIGURE 6 The BET specific surface area of (a) CeO_2/CuO and (b) CeO_2/CuO@N-GQDs@NH_2

TABLE 1 BET surface area (S_{BET}) and the total pore volumes (V_{total}) of the nanostructures

Materials	S_{BET} (m^2/g)	V_{total} (cm^3/g)
CeO_2/CuO	1.72	0.04
CeO_2/CuO@N-GQDs	7.89	0.09
CeO_2/CuO@N-GQDs@NH_2	9.82	0.12

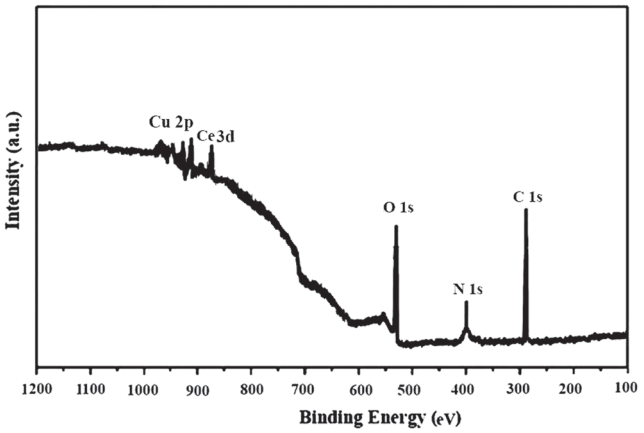

FIGURE 8 X-ray photoelectron spectroscopy (XPS) analysis of CeO_2/CuO@GQDs@NH_2 nanocomposite

Figure 8. In the wide-scan spectrum of the nanocatalyst, the predominant components are Cu 2p (940–970 eV), Ce 3d (883.8 eV), O 1 s (530.6 eV), N 1 s (400 eV) and C 1 s (286.3 eV).

Initially, we investigated the three-component reaction of benzaldehyde, malononitrile and 2-hydroxy-1,-4-naphthaquinone as a model reaction. The model reactions were performed using *p*-TSA, $NaHSO_4$, ZrO_2, Et_3N, CeO_2/CuO, CeO_2/CuO@N-GQDs and CeO_2/CuO@N-GQDs@NH_2 nanocomposites. The reactions were tested using various solvents including ethanol, acetonitrile, water and dimethylformamide. The best results were obtained in EtOH and the reaction gave convincing results in the presence of CeO_2/CuO@N-GQDs@NH_2 nanocomposite (6 mg) under reflux conditions (Table 2). In further studies on the catalyst loading, we recognized that the yield of compound **4d** remained almost the same when 7 mg of CeO_2/CuO@N-GQDs@NH_2

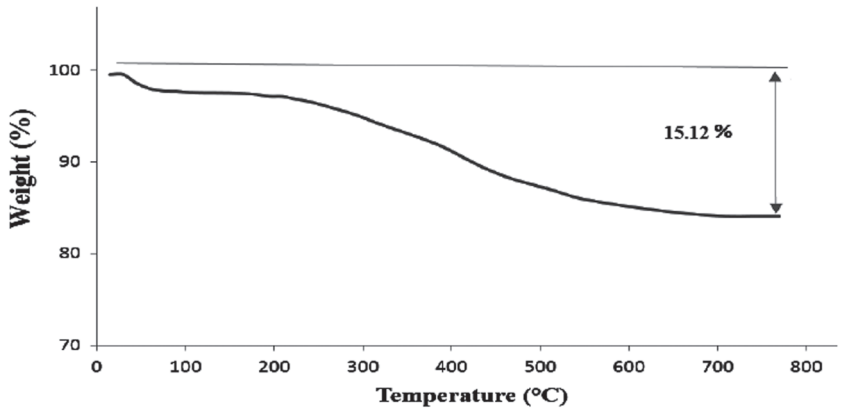

FIGURE 7 Thermogravimetric analysis of CeO_2/CuO@N-GQDs@NH_2

TABLE 2 Optimization of reaction conditions using different catalysts[aa]

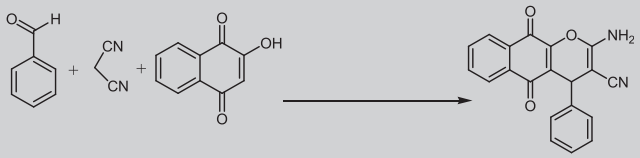

Entry	Catalyst (amount)	Solvent (reflux)	Time (min)	Yield[ab] (%)
1	None	EtOH	400	NR
2	*p*-TSA (5 mol%)	EtOH	400	10
3	$NaHSO_4$ (6 mol%)	EtOH	350	21
4	ZrO_2 (5 mol%)	EtOH	350	32
5	Et_3N (5 mol%)	EtOH	400	60
6	CeO_2/CuO nanocomposite	EtOH	250	48
7	CeO_2/CuO@N-GQDs nanocomposite	EtOH	150	70
8	CeO_2/CuO@N-GQDs@NH_2 nanocomposite (5 mg)	EtOH	75	86
9	CeO_2/CuO@N-GQDs@NH_2 nanocomposite (6 mg)	EtOH	75	90
10	CeO_2/CuO@N-GQDs@NH_2 nanocomposite (7 mg)	EtOH	75	90
11	CeO_2/CuO@N-GQDs@NH_2 nanocomposite (6 mg)	H_2O	120	70
12	CeO_2/CuO@N-GQDs@NH_2 nanocomposite (6 mg)	DMF	100	75
14	CeO_2/CuO@N-GQDs@NH_2 nanocomposite (6 mg)	CH_3CN	80	80

[a]Benzaldehyde (1 mmol), malononitrile (1 mmol) and 2-hydroxy-1,4-naphthaquinone (1 mmol).
[b]Isolated yield.

nanocomposite was used. The use of lower catalyst loading (5 mg) afforded **4d** in 86% yield.

The influence of electron-withdrawing and electron-donating substituents on the aromatic ring of aldehydes upon the reaction yields was investigated. The results showed excellent in yields from aromatic aldehydes, either bearing electron-withdrawing or electron-donating substituents (Table 3). Aromatic aldehydes having NO_2 and halogen groups reacted at a faster rate compared with aromatic aldehydes substituted with other groups.

Generalization of the reaction was carried out by employing various aldehydes, malononitrile or ethyl cyanoacetate, and the results are summarized in Table 3. The structures of the prepared benzo[g]chromenes were fully characterized by ^1H and ^{13}C NMR spectra, IR spectra and elemental analysis. For example, in the ^1H NMR spectrum of **4d**, the proton at 4.61 ppm displays CH aliphatic. The protons at 7.29–7.84 ppm indicate CH aromatic and NH_2. In the FT-IR spectrum of **4d**, the peaks at 3457 and 3392 cm^{-1} are related to the stretching vibrational absorptions of N–H; the peaks at 2213 and 1662 cm^{-1} are related to the stretching vibrational absorptions of C ≡ N and C=O respectively.

To compare the efficiency of CeO_2/CuO@N-GQDs@NH_2 nanocomposite with the reported catalysts for the synthesis of benzo[g]chromenes, the results are tabulated in Table 4. As the table shows, CeO_2/CuO@N-GQDs@NH_2 nanocomposite is superior with respect to the reported catalysts in terms of reaction time, yield and conditions.

We considered recycling of CeO_2/CuO@N-GQDs@NH_2 nanocomposite as a catalyst for the model reaction. The results showed that nanocomposite can be reused several times without remarkable loss of catalytic activity (yields 90–88%; Figure 9).

The morphology of CeO_2/CuO@N-GQDs@NH_2 nanocomposite was investigated by scanning electron microscopy (SEM) before use and after reuse five times (Figure 10). The shape and size of the nanoparticles remained unchanged before and after reaction. We suppose that this is also a possible reason for the extreme stability of the nanocatalyst presented herein.

To complete the reusability studies, we have used the hot filtration test.[37] For this purpose, we studied the model reaction three-component reaction of benzaldehyde, malononitrile and 2-hydroxy-1,4-naphthaquinone under optimized conditions. The reaction mixture was filtered after 50% conversion to remove the catalyst. Continuation of the reaction under the same conditions showed 54% conversion after 2.5 h. This result shows that the

TABLE 3 Synthesis of benzo[g]chromenes using CeO_2/CuO@N-GQDs@NH_2 nanocomposite (6 mg) under reflux conditions[aa]

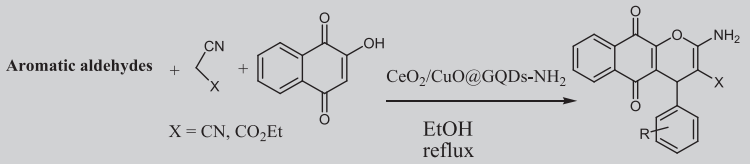

Entry	Aldehyde (1a–1l)	Malononitrile or ethyl cyanoacetate	Product (4a–4l)	Time (min)	Yield[b] (%)	m.p. (°C)[(reference)]	m.p. (°C) (reported)
1	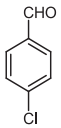		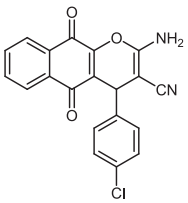 **4a**	65	93	249–252[10]	249–252
2	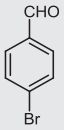		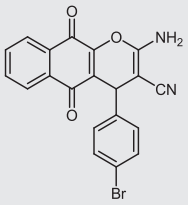 **4b**	65	92	253–255[10]	253–255
3	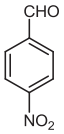		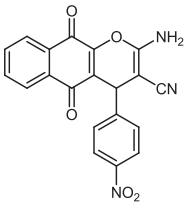 **4c**	65	94	234–235[10]	240–242
4			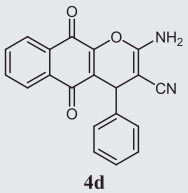 **4d**	75	90	261–262[10]	261–262

(Continues)

TABLE 3 (Continued)

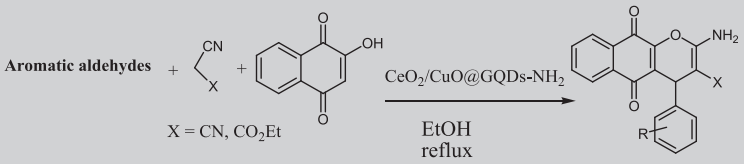

Entry	Aldehyde (1a–1l)	Malononitrile or ethyl cyanoacetate	Product (4a–4l)	Time (min)	Yield[b] (%)	m.p. (°C)[(reference)]	m.p. (°C) (reported)
5			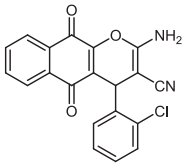 **4e**	65	92	236–239[10]	237–239
6	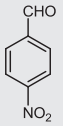		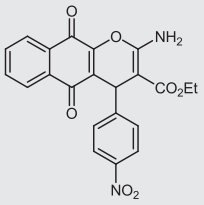 **4f**	80	91	197–199[39]	197–199
7	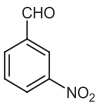		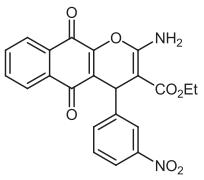 **4g**	90	85	198–200[40]	198–200
8	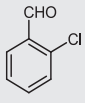		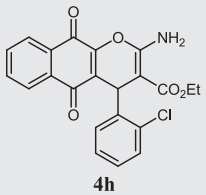 **4h**	100	87	208–210[40]	208–210

(Continues)

TABLE 3 (Continued)

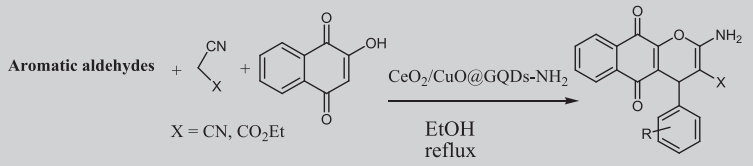

Entry	Aldehyde (1a–1l)	Malononitrile or ethyl cyanoacetate	Product (4a–4l)	Time (min)	Yield[b] (%)	m.p. (°C)[(reference)]	m.p. (°C) (reported)
9	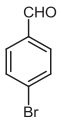		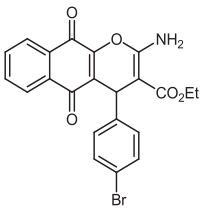 **4i**	90	87	190–192[40]	190–192
10	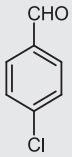		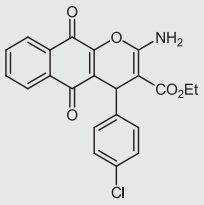 **4j**	90	88	189–191[16]	198–200
11	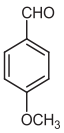		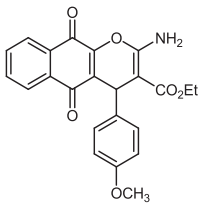 **4k**	120	80	224–226[39]	223–225
12	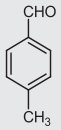		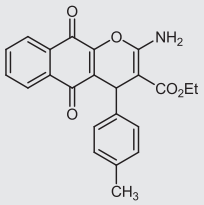 **4l**	120	83	211–214[16]	212–24

(Continues)

TABLE 3 (Continued)

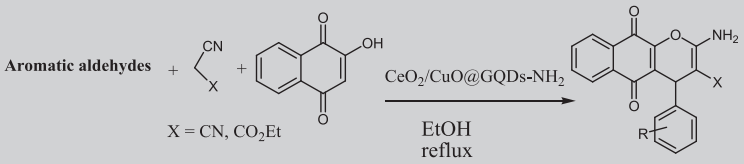

Entry	Aldehyde (1a–1l)	Malononitrile or ethyl cyanoacetate	Product (4a–4l)	Time (min)	Yield[b] (%)	m.p. (°C)[(reference)]	m.p. (°C) (reported)
13	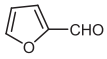		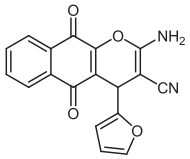 4m	90	84	—	192–194
14	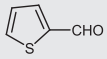		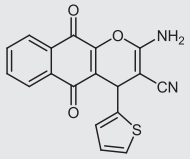 4n	100	84	—	186–188

[a]Aromatic aldehydes (1 mmol), malononitrile or ethyl cyanoacetate (1 mmol) and 2-hydroxy-1,4-naphthaquinone (1 mmol).
[b]Isolated yield.

TABLE 4 Comparison of catalytic activity of CeO_2/CuO@N-GQDs@NH_2 nanocomposite with other reported catalysts for the synthesis of **4d**

Entry	Catalyst (condition)	Time (min)	Yield[aa] (%)	Reference
1	Lipase (20 mg, 55°C, EtOH)	800	85	[8]
2	Et_3N (10 mol%,CH_3CN)	900	82	[10]
3	DBU (10 mol%, H_2O, reflux)	90	87	[13]
4	TEBA (10 mol%, 85°C)	240	90	[15]
5	CeO_2/CuO@N-GQDs@NH_2 nanocomposite (6 mg, EtOH, reflux)	75	90	This work

[a]Isolated yield

amount of leaching of the catalyst into the reaction mixture should be low and confirms that the catalyst acts heterogeneously in the reaction.

To determine the degree of leaching of the metal from the heterogeneous catalyst, the catalyst was removed by filtration and the Ce and Cu amounts in the reaction medium after each reaction cycle were measured through inductively coupled plasma–atomic emission spectroscopy. The analysis of the reaction mixture by the inductively coupled plasma technique showed that the leaching of Ce and Cu was negligible (the leaching of Ce and Cu in five continuous runs was found to be ≤0.6 ppm).

A plausible mechanism for the preparation of benzo[g]chromenes using CeO_2/CuO@N-GQDs@NH_2 nanocomposites is indicated in Scheme 2. Firstly, we

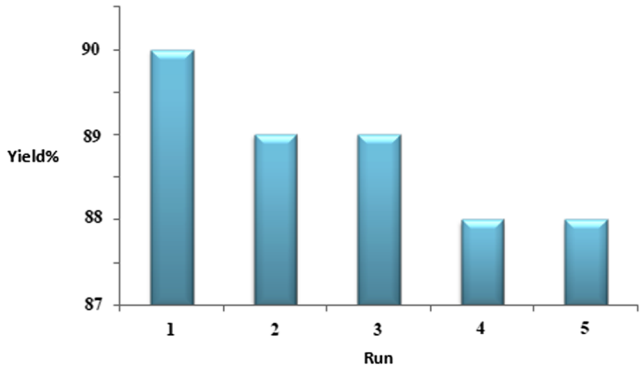

FIGURE 9 Recycling of CeO_2/CuO@N-GQDs@NH_2 nanocomposite as the catalyst for the model reaction

assumed that the reaction occurred via condensation between malononitrile and aldehyde, to form the intermediate **I** on the active sites of the CeO_2/CuO@N-GQDs@NH_2 nanocatalyst. Then, 2-hydroxy-1,-4-naphthaquinone was added to intermediate **I** to give the intermediate **II**. The intermediate **III** formed by intramolecular cyclization reaction. The migration of the hydrogen atom provided the final product (Scheme 2). The amino groups distributed on the surface of CeO_2/CuO@N-GQDs activated the C=O and C ≡ N groups through hydrogen bonding.[38–41] The activity of catalysts was influenced by the acid–base properties and many other factors such as surface area, geometric structure (particularly pore structure), the distribution of sites and the polarity of the surface sites.[38, 42] This mechanism is supported by the literature.[8, 11, 16]

A structure for the catalyst based on the results and some authoritative references[43–45] is presented in Figure 11. Herein, we reported the use of CeO_2/CuO@N-GQDs@NH_2 nanocomposite as a new efficient catalyst for the preparation of benzo[g]chromenes.

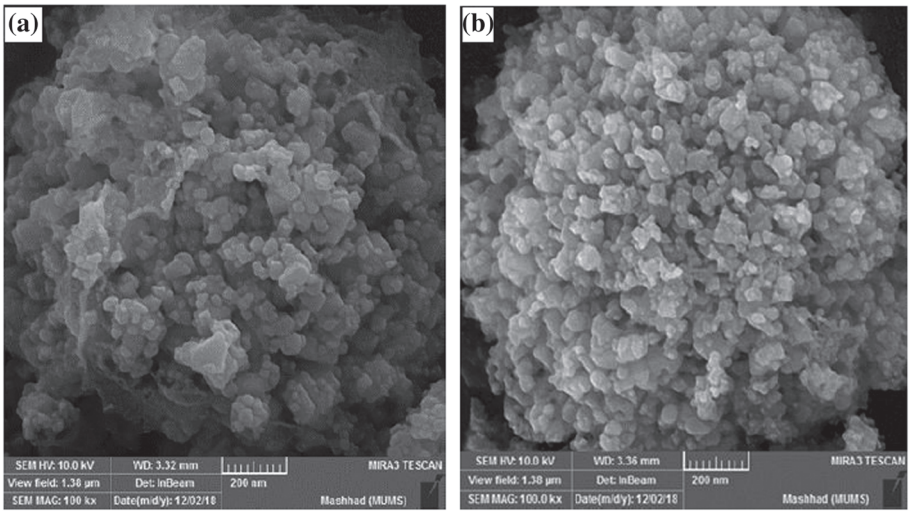

FIGURE 10 SEM images of CeO_2/CuO@N-GQDs@NH_2 nanocomposite (a) before use and (b) after reuse five times

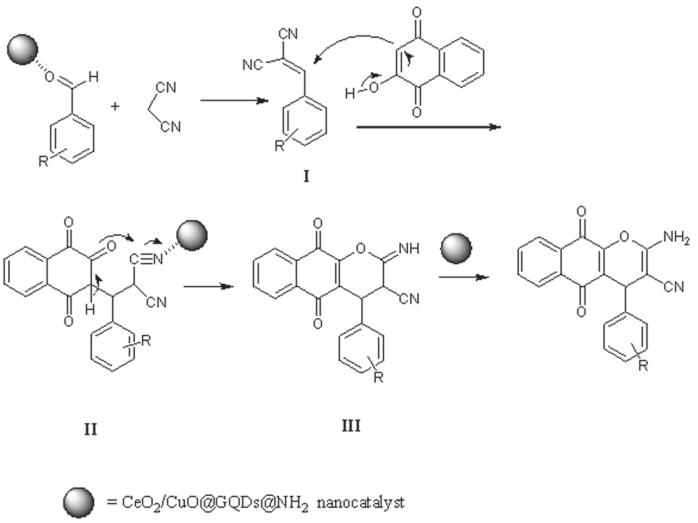

SCHEME 2 Proposed mechanism for the three-component reaction

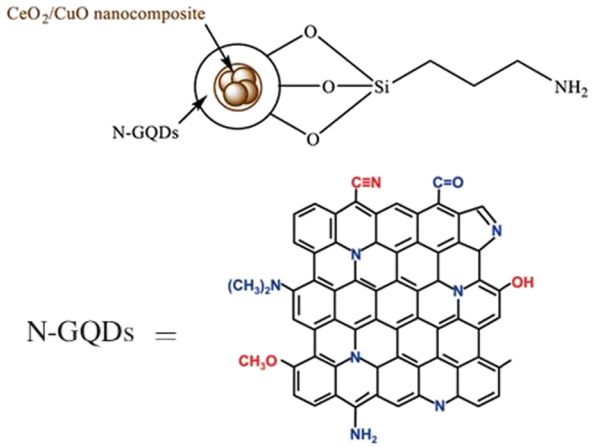

FIGURE 11 Structure for the CeO_2/CuO@N-GQDs@NH_2 nanocomposite

4 | CONCLUSIONS

In conclusion, we have reported an efficient method for the synthesis of benzo[g]chromenes using CeO_2/CuO@N-GQDs@NH_2 nanocomposite as a superior catalyst under reflux conditions. The new catalyst is characterized by SEM, TEM, FT-IR XRD, EDS, thermogravimetric analysis, XPS, BET and vibrating sample magnetometry. The current method provides obvious positive points including environmental friendliness, reusability of the catalyst, low catalyst loading and simple workup procedure.

ACKNOWLEDGMENTS

The authors are grateful to the University of Kashan for supporting this work.

ORCID

Javad Safaei-Ghomi https://orcid.org/0000-0002-9837-4478

REFERENCES

[1] M. S. L. Kumar, J. Singh, S. K. Manna, S. Maji, R. Konwar, G. Panda, *Bioorg. Med. Chem. Lett.* **2018**, *28*, 778.
[2] U. S. Rai, A. M. Isloor, P. Shetty, A. M. Vijesh, N. Prabhu, S. Isloor, M. Thiageeswaran, H. K. Fun, *Eur. J. Med. Chem.* **2010**, *45*, 2695.
[3] I. V. Ilyina, V. V. Zarubaev, I. N. Lavrentieva, A. A. Shtro, I. L. Esaulkova, D. V. Korchagina, S. S. Borisevich, K. P. Volcho, N. F. Salakhutdinov, *Bioorg. Med. Chem. Lett.* **2018**, *28*, 2061.
[4] S. T. Chung, W. H. Huang, C. K. Huang, F. C. Liu, R. Y. Huang, C. C. Wu, A. R. Lee, *Res. Chem. Intermed.* **2016**, *42*, 1195.
[5] S. Li, H. Xu, S. Cui, F. Wu, Y. Zhang, M. B. Su, Y. Gong, S. Qiu, H. Li, *J. Med. Chem.* **2016**, *59*, 6772.
[6] M. I. Fernández-Bachiller, C. Pérez, L. Monjas, J. Rademann, M. I. Rodríguez-Franco, *J. Med. Chem.* **2012**, *55*, 1303.
[7] N. Thomas, S. M. Zachariah, *Pharm. Clin. Res* **2013**, *6*, 11.
[8] F. Yang, H. Wang, L. Jiang, H. Yue, H. Zhang, Z. Wang, L. Wang, *RSC Adv.* **2015**, *5*, 5213.
[9] R. Ghahremanzadeh, T. Amanpour, A. Bazgir, *J. Heterocyclic Chem.* **2009**, *46*, 1266.
[10] A. Shaabani, R. Ghadari, S. Ghasemi, M. Pedarpour, A. H. Rezayan, A. Sarvary, S. W. Ng, *J. Comb. Chem.* **2009**, *11*, 956.
[11] J. Khalafy, S. Ilkhanizadeh, M. Ranjbar, *J. Heterocyclic Chem.* **2018**, *55*, 951.
[12] F. Khorami, H. R. Shaterian, *Res. Chem. Intermed.* **2015**, *41*, 3171.
[13] J. M. Khurana, B. Nand, P. Saluja, *Tetrahedron* **2010**, *66*, 5637.
[14] M. Perumal, P. Sengodu, S. Venkatesan, R. Srinivasan, M. Paramsivam, *Chem. Select.* **2017**, *2*, 5068.
[15] C. Yao, C. Yu, T. Li, S. Tu, *Chin. J. Chem.* **2009**, *27*, 1989.
[16] Y. Yu, H. Guo, X. Li, *J. Heterocyclic Chem.* **2011**, *48*, 1264.
[17] M. Misra, P. Kapur, M. K. Nayak, M. L. Singla, *New J. Chem.* **2014**, *38*, 4197.
[18] B. Xiao, Q. Zhao, D. Wang, G. Ma, M. Zhang, *New J. Chem.* **2017**, *41*, 8530.
[19] X. T. Zheng, A. Ananthanarayanan, K. Q. Luo, P. Chen, *Small* **2015**, *11*(14), 1620.
[20] B. Senel, N. Demir, G. Büyükköroglu, M. Yildiz, *Saudi. Pharm. J.* **2019**. https://doi.org/10.1016/j.jsps.2019.05.006
[21] M. J. Molaei, *RSC Adv.* **2019**, *9*, 6460.
[22] T. F. Yeh, C. Y. Teng, S. J. Chen, H. Teng, *Adv. Mater.* **2014**, *26*, 3297.
[23] F. Xi, J. Zhao, C. Shen, J. He, J. Chen, Y. Yan, K. Li, J. Liu, P. Chen, *Carbon* **2019**, *153*, 127.
[24] Y. Wang, Y. Shao, D. W. Matson, J. Li, Y. Lin, *ACS Nano* **2010**, *4*, 1790.
[25] Q. Li, S. Zhang, L. Dai, L. S. Li, *J. Am. Chem. Soc.* **2012**, *134*, 18932.
[26] A. L. M. Reddy, A. Srivastava, S. R. Gowda, H. Gullapalli, M. Dubey, P. M. Ajayan, *ACS Nano* **2010**, *4*, 6337.
[27] M. T. Hasan, R. Gonzalez-Rodriguez, C. Ryan, K. Pota, K. Green, J. L. Coffer, A. V. Naumov, *Nano Res.* **2019**, *12*, 1041.
[28] F. Temerov, A. Beliaev, B. Ankudze, T. T. Pakkanen, *J. Lumin.* **2019**, *206*, 403.
[29] S. Zhu, Y. Song, X. Zhao, J. Shao, J. Zhang, B. Yang, *Nano Res.* **2015**, *8*, 355.
[30] D. Qu, M. Zheng, J. Li, Z. Xie, Z. Sun, *Light Sci. Appl.* **2015**, *4*, 364.
[31] S. Sajjadi, A. Khataee, R. D. C. Soltani, A. Hasanzadeh, J. Phys, *Chem. Solids* **2019**, *127*, 140.
[32] Y. Du, S. Guo, *Nanoscale* **2016**, *8*, 2532.
[33] Y. Yan, J. Gong, J. Chen, Z. Zeng, W. Huang, K. Pu, J. Liu, P. Chen, *Adv. Mater.* **2019**, *31*. 1808283–1808305
[34] M. Li, T. Chen, J. J. Gooding, J. Liu, *ACS Sens.* **2019**. https://doi.org/10.1021/acssensors.9b00514
[35] Z. Wang, H. Zeng, L. Sun, J. Mater, *Chem. C* **2015**, *3*, 1157.
[36] D. Qu, M. Zheng, P. Du, Y. Zhou, L. Zhang, D. Li, H. Tan, Z. Zhao, Z. Xie, Z. Sun, *Nanoscale* **2013**, *5*, 12272.
[37] J. Chung, J. Kim, Y. Jang, S. Byun, T. Hyeon, B. M. Kim, *Tetrahedron Lett.* **2013**, *54*, 5192.

[38] J. Safaei-Ghomi, H. Shahbazi-Alavi, *J. Saudi Chem Soc.* **2017**, *21*, 698.
[39] J. Safaei-Ghomi, H. Shahbazi-Alavi, P. Babaei, H. Basharnavaz, S. G. Pyne, A. C. Willis, *Chem. Heterocycl. Compd* **2016**, *52*, 288.
[40] M. G. Dekamin, M. Eslami, A. Maleki, *Tetrahedron* **2013**, *69*, 1074.
[41] J. Safaei-Ghomi, N. Enayat-Mehri, F. Eshteghal, *J. Saudi Chem Soc.* **2018**, *22*, 485.
[42] J. Safaei-Ghomi, H. Shahbazi-Alavi, E. Heidari-Baghbahadorani, *RSC Adv.* **2014**, *4*, 50668.
[43] L. Luo, S. Ma, L. Li, X. Liu, J. Zhang, X. Li, D. Liu, T. You, *Food Chem.* **2019**, *292*, 98.
[44] X. Deng, J. Sun, S. Yang, H. Shen, W. Zhou, J. Lu, G. Ding, Z. Wang, *Appl. Phys. Lett.* **2015**, *107*, 241905.
[45] A. B. Ganganboina, A. D. Chowdhury, R. Doong, *Electrochim. Acta* **2017**, *245*, 912.

SUPPORTING INFORMATION

Additional supporting information may be found online in the Supporting Information section at the end of this article.

How to cite this article: Safaei-Ghomi J, Bateni F-S, Babaei P. CeO_2/CuO@N-GQDs@NH_2 nanocomposite as a high-performance catalyst for the synthesis of benzo[g]chromenes. *Appl Organometal Chem*. 2020;e5657. https://doi.org/10.1002/aoc.5657